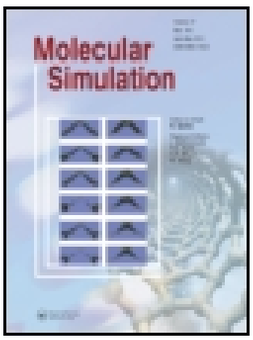

Molecular Simulation

ISSN: 0892-7022 (Print) 1029-0435 (Online) Journal homepage: https://www.tandfonline.com/loi/gmos20

Molecular dynamics simulations of the interaction of phospholipid bilayers with polycaprolactone

Mihaela Drenscko & Sharon M. Loverde

To cite this article: Mihaela Drenscko & Sharon M. Loverde (2019): Molecular dynamics simulations of the interaction of phospholipid bilayers with polycaprolactone, Molecular Simulation, DOI: 10.1080/08927022.2019.1606425

To link to this article: https://doi.org/10.1080/08927022.2019.1606425

MOLECULAR SIMULATION
https://doi.org/10.1080/08927022.2019.1606425

Taylor & Francis
Taylor & Francis Group

Molecular dynamics simulations of the interaction of phospholipid bilayers with polycaprolactone

Mihaela Drenscko[a,b,c] and Sharon M. Loverde[a,b,c]

[a]Department of Chemistry, College of Staten Island, City University of New York, New York, NY, USA; [b]Department of Physics, Graduate Center, City University of New York, New York, NY, USA; [c]Program in Chemistry, Biochemistry, and Physics, The Graduate Center of the City University of New York, New York, NY, USA

ABSTRACT

The molecular interaction between common polymer chains and the cell membrane is unknown. Molecular dynamics simulations offer an emerging tool to characterise the nature of the interaction between common degradable polymer chains used in biomedical applications, such as polycaprolactone, and model cell membranes. Herein we characterise with all-atomistic and coarse-grained molecular dynamics simulations the interaction between single polycaprolactone chains of varying chain lengths with a phospholipid membrane. We find that the length of the polymer chain greatly affects the nature of interaction with the membrane, as well as the membrane properties. Furthermore, we next utilise advanced sampling techniques in molecular dynamics to characterise the two-dimensional free energy surface for the interaction of varying polymer chain lengths (short, intermediate, and long) with model cell membranes. We find that the free energy minimum shifts from the membrane-water interface to the hydrophobic core of the phospholipid membrane as a function of chain length. Finally, we perform coarse-grained molecular dynamics simulations of slightly larger membranes with polymers of the same length and characterise the results as compared with all-atomistic molecular dynamics simulations. These results can be used to design polymer chain lengths and chemistries to optimise their interaction with cell membranes at the molecular level.

ARTICLE HISTORY
Received 11 September 2018
Accepted 8 April 2019

KEYWORDS
Phospholipid membrane; polycaprolactone; hydrophobic polymer; molecular dynamics

1. Introduction

The cell membrane acts as a selective permeability barrier, surrounding cells of living organisms. The membrane can allow the diffusion of certain hydrophobic molecules passively into the membrane, but block the entry of hydrophilic molecules. Self-assembled block copolymers in solution can act as common drug delivery vehicles [1] that are designed to transport small molecular cargo across the membrane barrier. A widely used, biodegradable polymer commonly used for drug delivery is polycaprolactone (PCL) [2–5]. PCL is also used for the design of other biomaterials such as stents [6] and is commonly used in tissue scaffolds [7]. PCL is a hydrophobic, semi-crystalline polymer [8,9]. However, the nature of the interaction between PCL polymers and the cell membrane is unknown. For example, it is unknown if a single PCL polymer itself can cross the cell membrane due to its hydrophobic nature; moreover, if the polymer is intercalated into the membrane, the polymer chains may affect the membrane properties, such as the ordering of the phospholipid tails, the area per lipid, and membrane thickness. Block copolymer interactions with the membrane have been shown to perturb and even porate the membrane using simulation studies [10–12]. In this study, we focus on the molecular level characterisation of the interaction of hydrophobic polymers such as PCL with model cell membranes such as POPC using both large-scale all-atomistic and coarse-grained simulations. POPC (1-palmitoyl-2-oleoyl-sn-glycero-3-phosphocholine) is chosen since it is a model lipid found in the cell membrane and is commonly used for biophysical measurements. PCL is a biodegradable, hydrophobic polymer that has been approved by the Food and Drug Administration (FDA) widely used in biomaterial applications [6] due to its gradual hydrolysis to monomers [13]. A variety of hydrophobic drugs have been encapsulated within PCL self-assemblies for controlled release and targeted drug delivery, such as the anti-cancer drug paclitaxel [14]. Furthermore, the shape of the self-assembled structure has been shown to influence the solubility of the hydrophobic drug in the hydrophobic environment of a micelle core [15].

Herein we describe results of both long-time all-atomistic and coarse-grained molecular dynamics simulations of single polycaprolactone (PCL) chains of varying lengths interacting with model POPC phospholipid membranes. We find that the nature of the interaction of the PCL chain with the lipid membrane varies as a function of chain length, finding that shorter chains prefer to sit at the membrane-water interface while longer chains prefer to behave as slightly distended hydrophobic globules in the centre of the hydrophobic lipid membrane core. We find that this variation of the strength of interaction by polymer length also affects the membrane properties, such as area per lipid and membrane width. Surprisingly, we find that shorter chain lengths thin the membrane the most during the length of these simulation studies. We next characterise the complete interaction free

CONTACT Sharon M. Loverde sharon.loverde@csi.cuny.edu
Supplemental data for this article can be accessed at https://doi.org/10.1080/08927022.2019.1606425

energy surface of the polymer with the membrane using advanced sampling techniques in molecular dynamics, namely metadynamics [16]. Advanced sampling techniques such as metadynamics, umbrella sampling [17], and ABF (Adaptive Biasing Force methodology) [18] are emerging tools in molecular dynamics simulations that have been used to probe the interaction of small molecules with model membranes [19]. We have previously used metadynamics to characterise the collapse of single hydrophobic chains of PS (polystyrene) in water [20]. In this case, to characterise the interaction free energy surface for PCL with the model phospholipid membrane composed by POPC, we choose to characterise the interaction free energy as a function of two separate collective variables: radius of gyration of the polymer and the distance between centre of masses of the POPC membrane and the PCL chains. We find results that are consistent with previously described long-time all-atomistic simulations studies, with the free energy minimum that shifts from the membrane-water interface to the centre of the hydrophobic inner core of the phospholipid membrane as a function of polymer chain length.

Next, all-atom molecular dynamics (MD) simulations are used to build a coarse grain (CG) model of polycaprolactone (PCL) interacting with the same phospholipid bilayer (POPC) to compare the results of all-atomistic molecular dynamics simulations with coarse grain molecular dynamics simulations. We find that the partitioning and conformation of the polymer in the membrane again depend on length. The collapsed conformation of shorter chains agrees well with all-atomistic molecular dynamics simulations however intermediate and longer chains reach a more extended conformation in coarse grain simulations as compared with all-atomistic simulations. These results may be dependent on the finite size of the membrane as well as the method for parameterisation of the interaction between the CG PCL polymer and the CG phospholipids. In order to further improve the present model, parameters could be refined such that agreement is found between all-atomistic and coarse grain surface tensions. Nevertheless, with all simulations outlined we gain fundamental insight into the qualitative trend in the interaction behaviour of single hydrophobic polymers with phospholipid membranes.

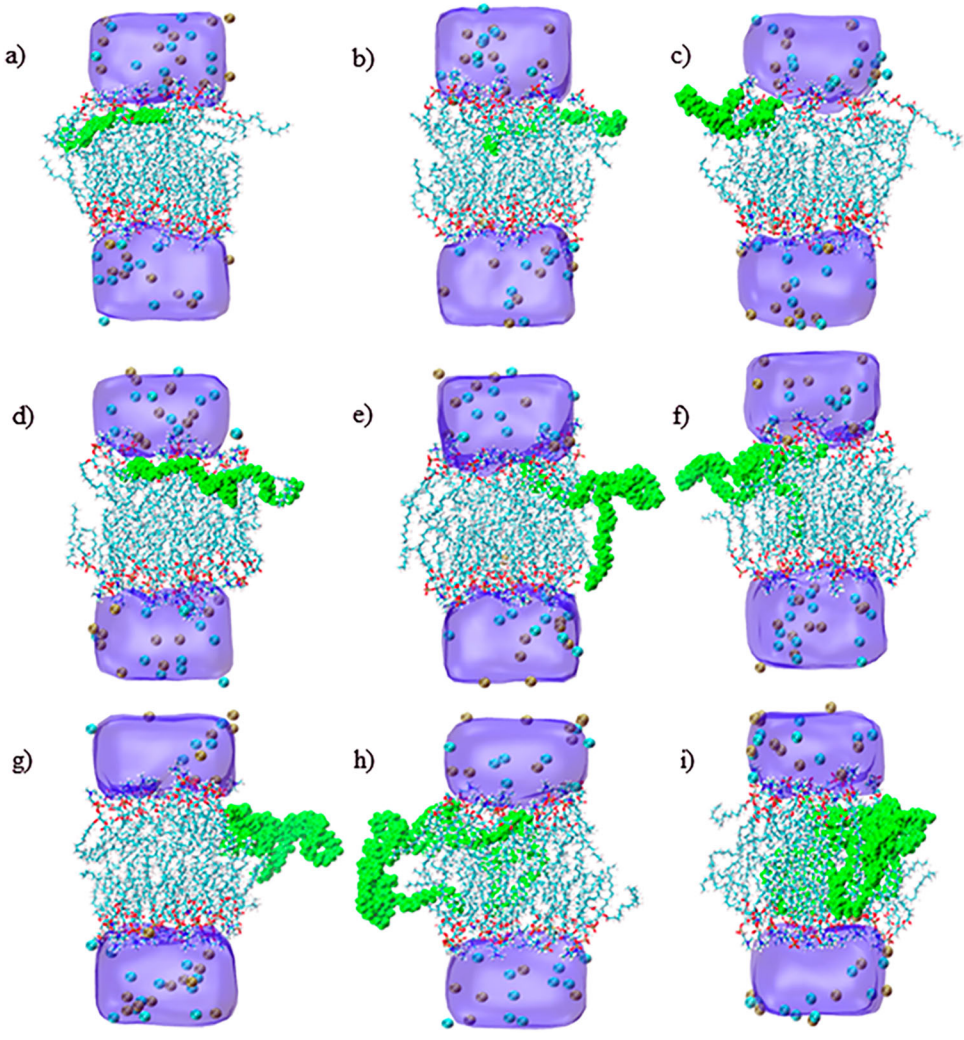

Figure 1. (Colour online) Snapshots of varying lengths of PCL chains in a POPC membrane at the end of 150 ns simulation: (a) 5 PCL; (b) 8 PCL; (c) 10 PCL; (d) 13 PCL; (e) 17 PCL; (f) 22 PCL; (g) 30 PCL; (h) 44 PCL; (i) 58 PCL. The polymer chain, potassium and chloride ions are displayed in a van der Waals representation while POPC membrane chains are displayed in a CPK representation. Water is indicated by a transparent cyan background.

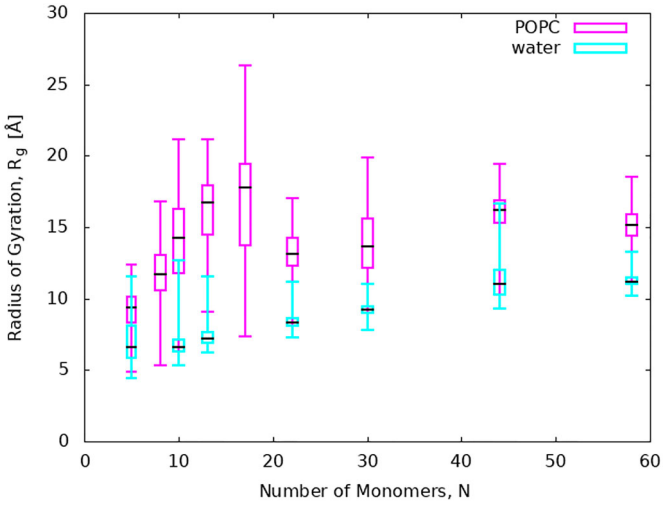

Figure 2. (Colour online) Comparison of last 100 ns PCL radius of gyration versus number of monomers for single PCL chains in POPC (150 ns total simulation time) and last 5 ns average PCL radius of gyration versus number of monomers for PCL in water (50 ns total simulation time) using a boxplot representation.

2. Methods

All-atomistic. The all-atomistic POPC bilayer membrane systems consisted of 59 POPC and approximately 3000 TIP3P water molecules containing nine different monomer chain lengths of polycaprolactone (5,8,10,13,17,22,30,44 and 58 monomers) (Supplementary Table 1) simulated with a 0.2 M concentration of KCl salt in solution for the time period of 150 ns each after being initially equilibrated at $T = 300$ K for 50 ns. Force field parameters were based on CHARMM27 [21,22] for PCL. The CHARMM TIP3P model [23] was used for water. The CHARMM36 force field was used for POPC [24]. Simulations were performed with the NAMD2 software package [25,26]. All systems used the NPT ensemble and Langevin dynamics [27] at a temperature of 300 K with a damping coefficient $\gamma = 5$ ps^{-1}, at a pressure of 1 atm using an anisotropic Langevin piston method with a piston period of 200 fs and a damping time scale of 50 fs. The SHAKE algorithm was used to hold covalent bonds involving hydrogen rigid, allowing a 2 fs time step. The Particle Mesh Ewald (PME) algorithm [28] was employed to take full electrostatic interactions into account, with full periodic boundary conditions. The cut-off for van der Waals interactions was 12 Å with a smooth switching function at 10 Å used to truncate the van der Waals potential energy at the cut-off distance. Coordinates were saved every 2 ps for the trajectory analysis.

Coarse-grained. In addition to the above, CG molecular dynamics simulations of CG PCL [15] interacting with a zwitterionic lipid membrane were run using the SDK force field parameters for phospholipids, specifically POPC [29]. Single CG PCL chains of sizes 5,8,10,13,17,22,30,44,58,72,86 and 100 monomers were first equilibrated in water for up to 20 ns. The POPC membrane consisted of 236 CG lipids surrounded by 7024 CG waters. For a summary of system sizes and setups see Supplementary Table 2. For details concerning the parameterisation and models of PCL or zwitterionic lipids, we refer the reader to earlier publications [15,29] as well as to Supplementary Tables 3–6. Intramolecular (bond, angle parameters) for CG PCL were obtained from AA simulations of PCL chains at 1atm and 300 K as described in Loverde et al. [15]. All CG simulations were run using LAMMPS [30], a parallel molecular dynamics code developed by Sandia National Laboratory, with a timestep of 10 fs. The temperature and the pressure were controlled using the Nose–Hoover [31] algorithm at 300 K and 1 atm. For the electrostatic interactions, we used a particle–particle–particle mesh (PPPM) [32]. The Lennard-Jones pair potential cut-off distance was set to 15 Å. The system was run initially in the canonical (NVT) ensemble for 1 ns at 300 K, then for 150 ns in isothermal-isobaric (NPT) ensemble also at 300 K and 1 bar pressure with a drag factor of 0.01 added to the barostat.

Free energy calculations. All-atomistic two-dimensional metadynamics simulations were run for 150 ns for three different polymer lengths (5,17, and 58 monomers) using the Collective Variables Module [33,34] in NAMD2 using the radius of gyration of the polymer chain and the centre of mass distance between the PCL chain and the phospholipid headgroups as collective variables. Metadynamics [16] is a methodology whereby a Gaussian potential is applied with time to the free energy surface

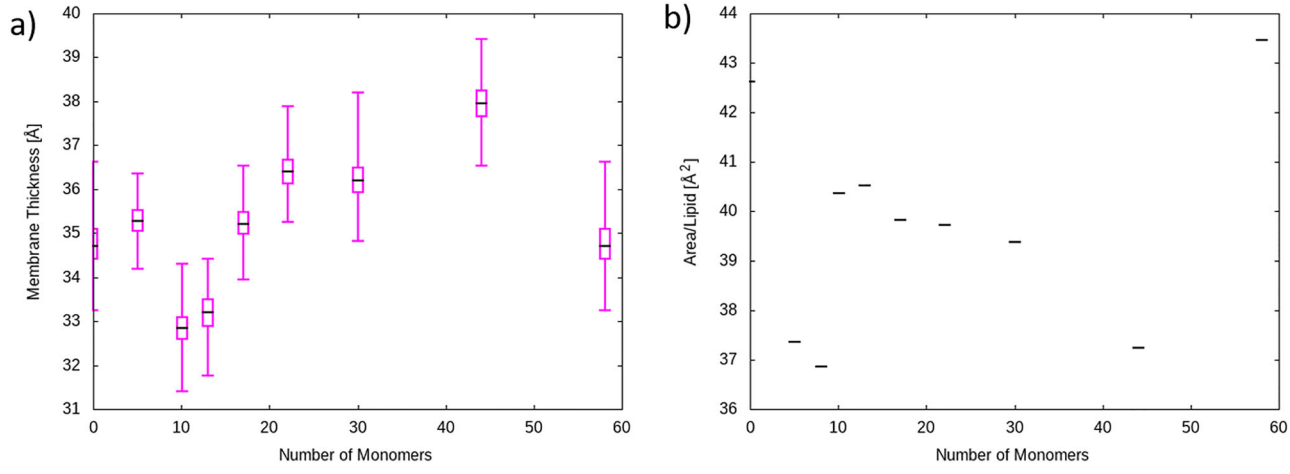

Figure 3. (Colour online) Membrane thickness and area per lipid. (a) Last 100 ns POPC membrane thickness versus number of monomers for single PCL chains in POPC. (b) Last 100 ns POPC area/lipid versus number of monomers for single PCL chains in POPC. Both displayed using a boxplot representation.

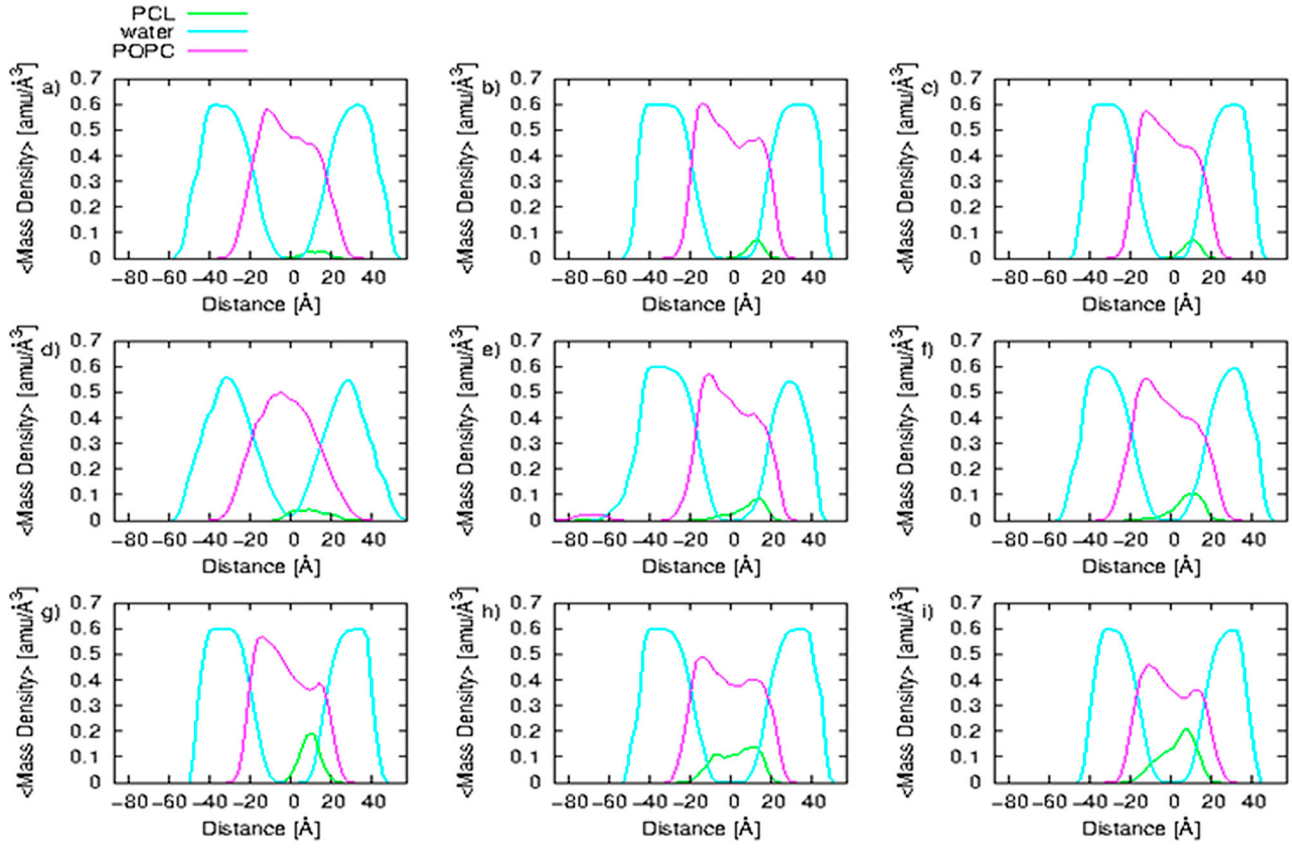

Figure 4. (Colour online) Average mass density distributions of the PCL (green), water (cyan) and POPC (magenta) along the *Z*-axis of the simulation box, for the last 10 ns of simulations. (a) 5 PCL (b) 8 PCL (c) 10 PCL (d) 13 PCL (e) 17 PCL (f) 22 PCL (g) 30 PCL (h) 44 PCL (i) 58 PCL.

until it can overcome free energy minima. Metadynamics has been extensively applied to an accurate sampling of the free energy surfaces of protein configurations [35], chemical reaction pathways [36], and other phenomena. Briefly, in metadynamics, an additional potential V_{meta} on a set of collective variables, ξ, such that $V_{meta}(\xi(t)) = \sum_{t'=\delta t,2\delta t,\ldots}^{t'<t} W \prod_{i=1}^{N_{cv}} \exp(-(\xi_i(t)-\xi_i(t'))^2/2\sigma_{\xi_i}^2)$ [16]. During simulation, if the system is sampling for long enough, the effective potential of mean force becomes constant and $-V_{meta}(\xi)$ becomes an estimate of the potential of mean force, $A(\xi) - V_{meta}(\xi) + C$. Metadynamics parameters of hill energy (hill weight, W) were set to 0.01 kcal/mol, hill creation frequency, (i.e. integration steps required for addition of a new hill to the metadynamics potential, δt) was set to 100, and radius of gyration fluctuation amplitude $\sigma_\xi$was set to 0.5 Å and centre of mass fluctuation amplitude σ_ξ was set to 10 Å.

3. Results and discussion

All-atomistic simulations. We highlight the chain conformation at the end of the simulation time period as shown in Figure 1 for all polymer chain lengths (5,8,10,13,17,22,30,44 and 58 monomers). Clearly, we see a trend that for short chains, the PCL chain is in an extended conformation close to the phospholipid membrane-water interface as shown in Figure 1(a,b) for chain lengths of 5,8 monomers. For intermediate chain lengths (10,13,17,22,30 monomers) the polymer chain moves

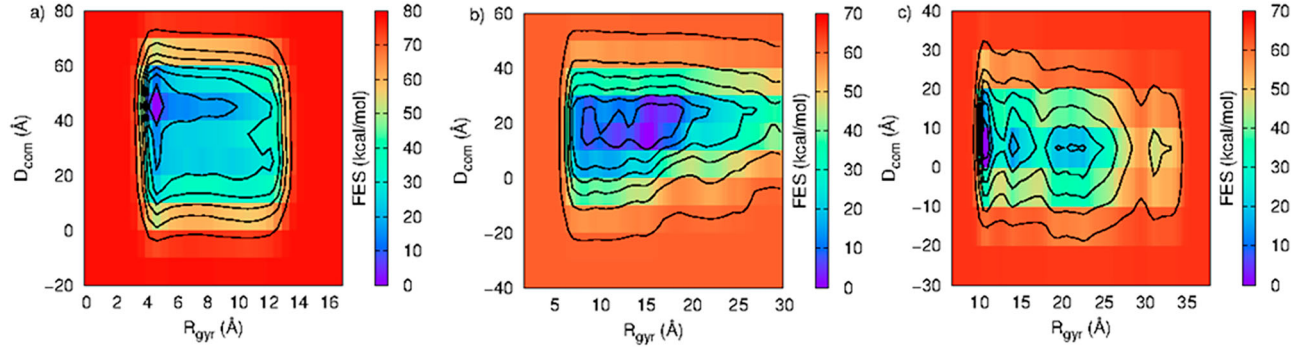

Figure 5. (Colour online) All-atomistic metadynamics (150 ns) 2D free energy distribution contour graphs as a function of the D_{com}, distance between the centre of mass of the phospholipid head groups and the centre of mass of the polymer, and of the R_{gyr}, radius of gyration of the polymer. PCL placed in POPC membrane: (a) 5 PCL (b) 17 PCL (c) 58 PCL.

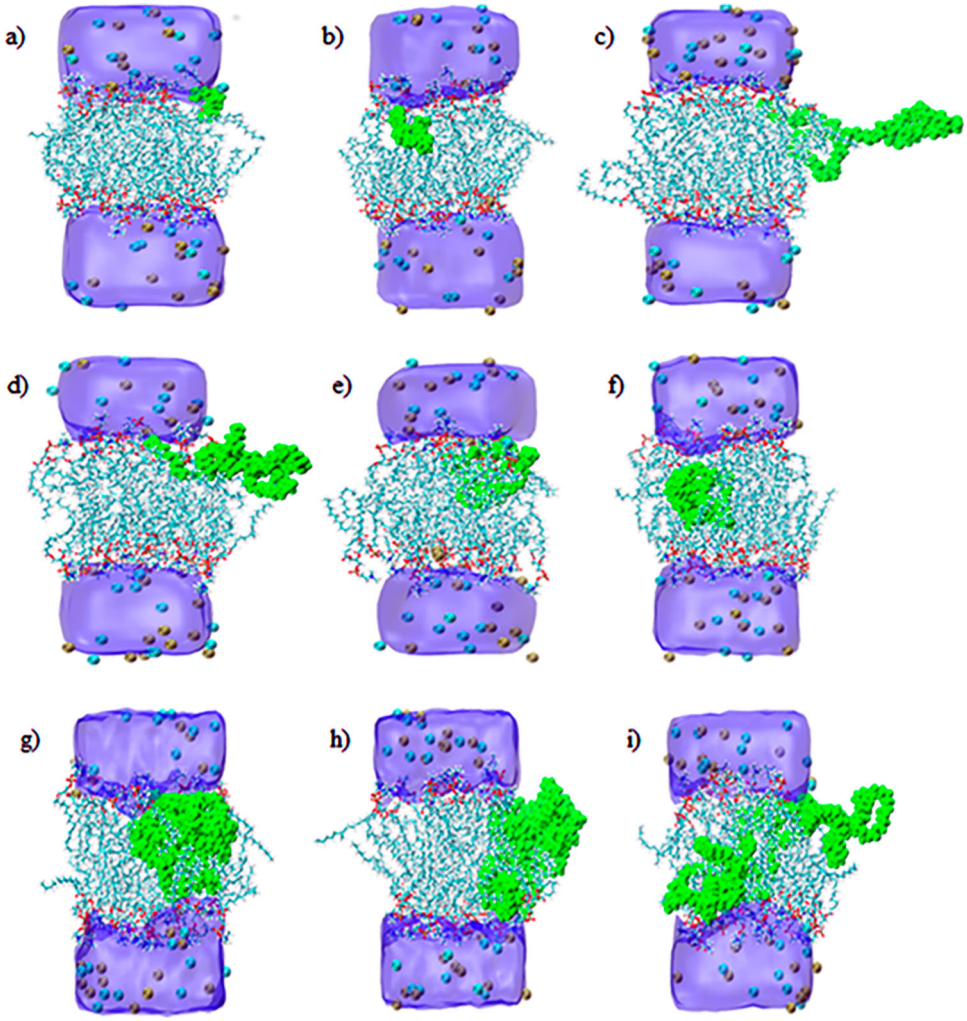

Figure 6. (Colour online) Snapshots for all-atomistic metadynamics simulations, showing the PCL polymer chain conformation in the energy wells. For (a,b), the conformation of a 5 monomer PCL chain in the energy well at (a) 0 kcal/mol; (b) 14.66 kcal/mol. For (c–f) the conformation of a 17 monomer PCL chain in the energy well at (c) 0 kcal/mol; (d) 5.32 kcal/mol; (e) 7.48 kcal/mol; (f)12.17 kcal/mol. For (g)–(i) the conformation of a 58 monomer PCL chain in the energy well at (g) 0 kcal/mol; (h) 14.79 kcal/mol; (i)18.39 kcal/mol.

towards the membrane interface, however, chain ends wrap around or else intercalate into the centre of the hydrophobic core of the membrane as shown in Figure 1(c–g). For the longest chain lengths as shown in Figure 1(h,i) the chain remains in a collapsed conformation that slightly opens up and maintains contacts with the membrane-water interface. Overall, we find that – for the timescales simulated – shorter PCL chains move towards the membrane-water interface in an extended conformation, while longer chains remain in a more collapsed conformation in the centre of the phospholipid membrane.

We next characterise the size of the PCL chain by calculating its radius of gyration (R_g) and end-to-end distance (R_e) and averaging over the last 100 ns simulation time for the range of chain lengths from 5 to 58 monomers. Comparing R_g for PCL in the membrane and PCL in water as a function of chain length as shown in Figure 2, there is a clear trend. For longer chain sizes of more than 20 monomers, R_g values are higher for the simulation performed for PCL surrounded by a POPC membrane environment (Figure 2) compared with the simulations in which PCL is simulated in water (a poor solvent). This trend is also true for smaller and intermediate chain lengths. The R_g of the PCL chain is always larger in the POPC membrane than in pure water. For smaller chains (5,8,10,13,17 monomers PCL), R_g average increases with the number of monomers in the chain, from 8.96 to 17.83 Å. Longer chains (22,30,44,58 monomers PCL), however, display a decrease in average R_g, with values close to each other, fluctuating around 15 Å. This tendency is also observed for PCL in water, for longer chains leveling of R_g around 10 Å. While PCL chains evolve to a globular state when placed in water, the POPC membrane environment opens up the collapsed globule, with smaller chains opening up to an extended conformation and moving towards the interface as shown in Figure 1.

When single PCL chains are inserted into the membrane, the effect of the polymer chain on membrane thickness varies according to the chain length as shown in Figure 3(a). Small (8,10 monomers PCL) chains cause a slight thinning of the membrane, from an average ~ 35 Å without polymer chains to ~ 33 Å for an 8 monomer chain. Longer chains, however, display an increase in membrane thickness, as compared to intermediate length chains, with an increase ~ 39 Å for a 44 monomer chain. On the contrary, the smallest chain lengths thin the membrane. They are completely absorbed to the interface, in an extended conformation (Figure 1).

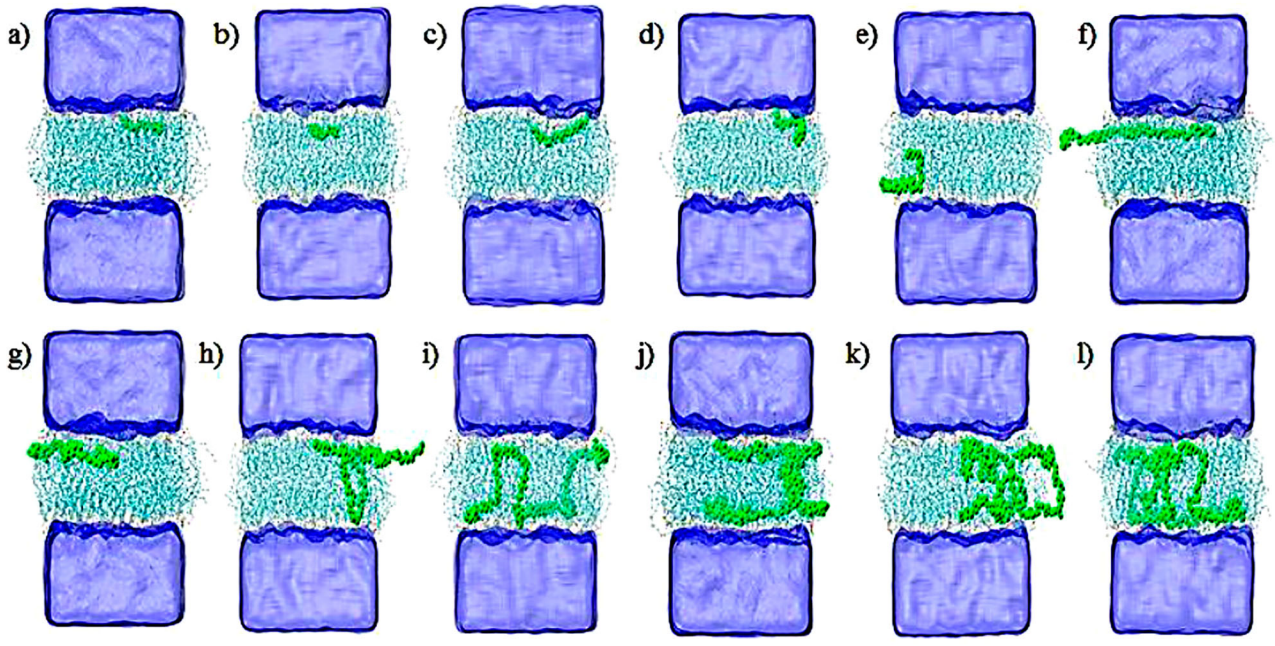

Figure 7. (Colour online) Snapshots of coarse-grained PCL in a POPC membrane at the end of 150 ns simulation PCL: (a) 5 PCL; (b) 8 PCL; (c) 10 PCL; (d) 13 PCL; (e) 17 PCL; (f) 22 PCL; (g) 30 PCL; (h) 44 PCL; (i) 58 PCL; (j) 72 PCL; (k) 86 PCL; (l) 100 PCL. The polymer chain, potassium and chloride ions are displayed in a van der Waals representation while POPC membrane chains are displayed in a CPK representation. Water is indicated by transparent conformation background.

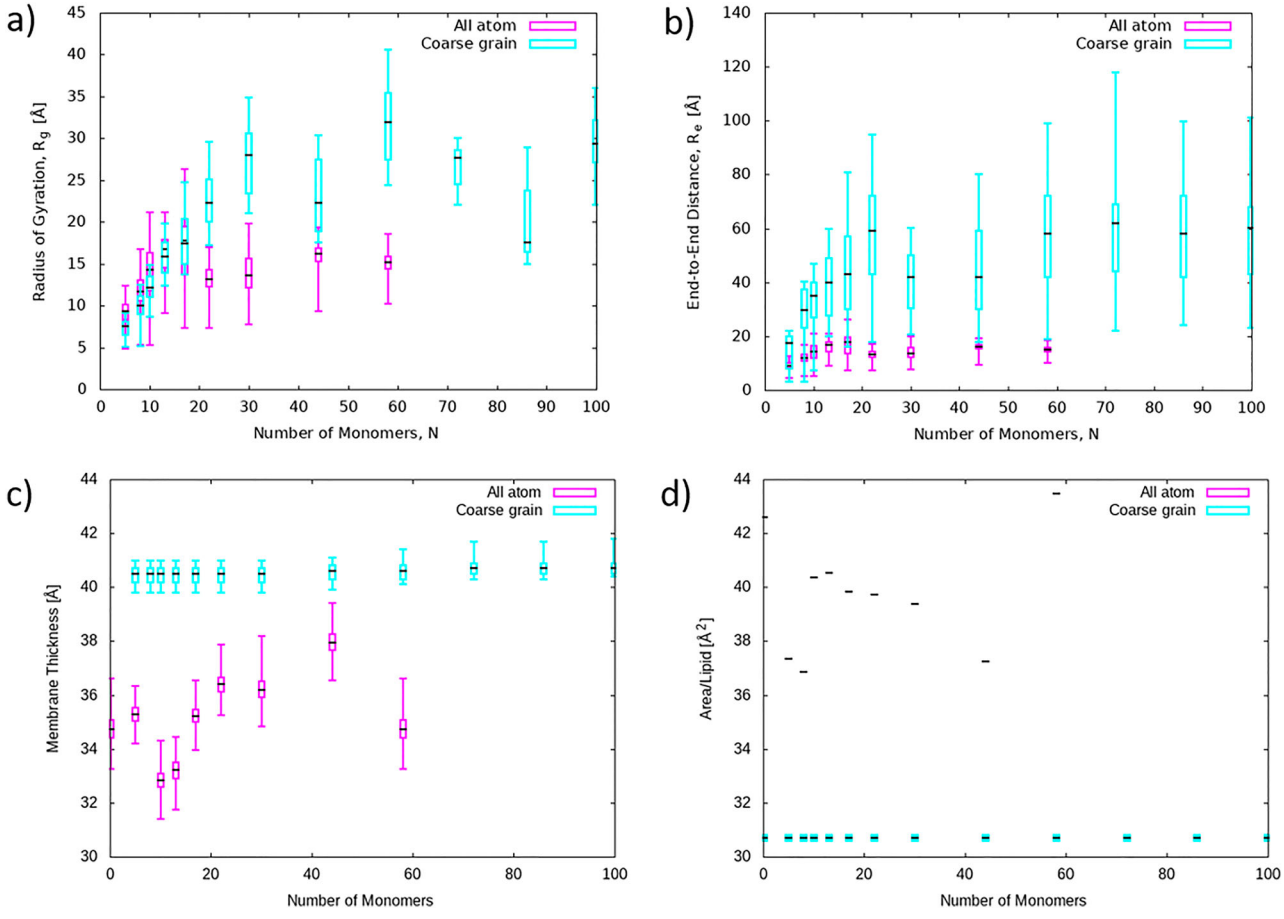

Figure 8. (Colour online) (a) AA-CG comparison of last 100 ns average PCL radius of gyration versus number of monomers for single PCL chains in POPC membrane. (b) AA-CG comparison of last 100 ns average PCL end-to-end distance versus number of monomers for single PCL chains in a POPC membrane. (c) AA-CG comparison of last 100 ns average membrane thickness versus number of monomers for single PCL chains in POPC membrane. (d) AA-CG comparison of last 100 ns average area per lipid versus number of monomers for single PCL chains in POPC membrane. All displayed in boxplot representation.

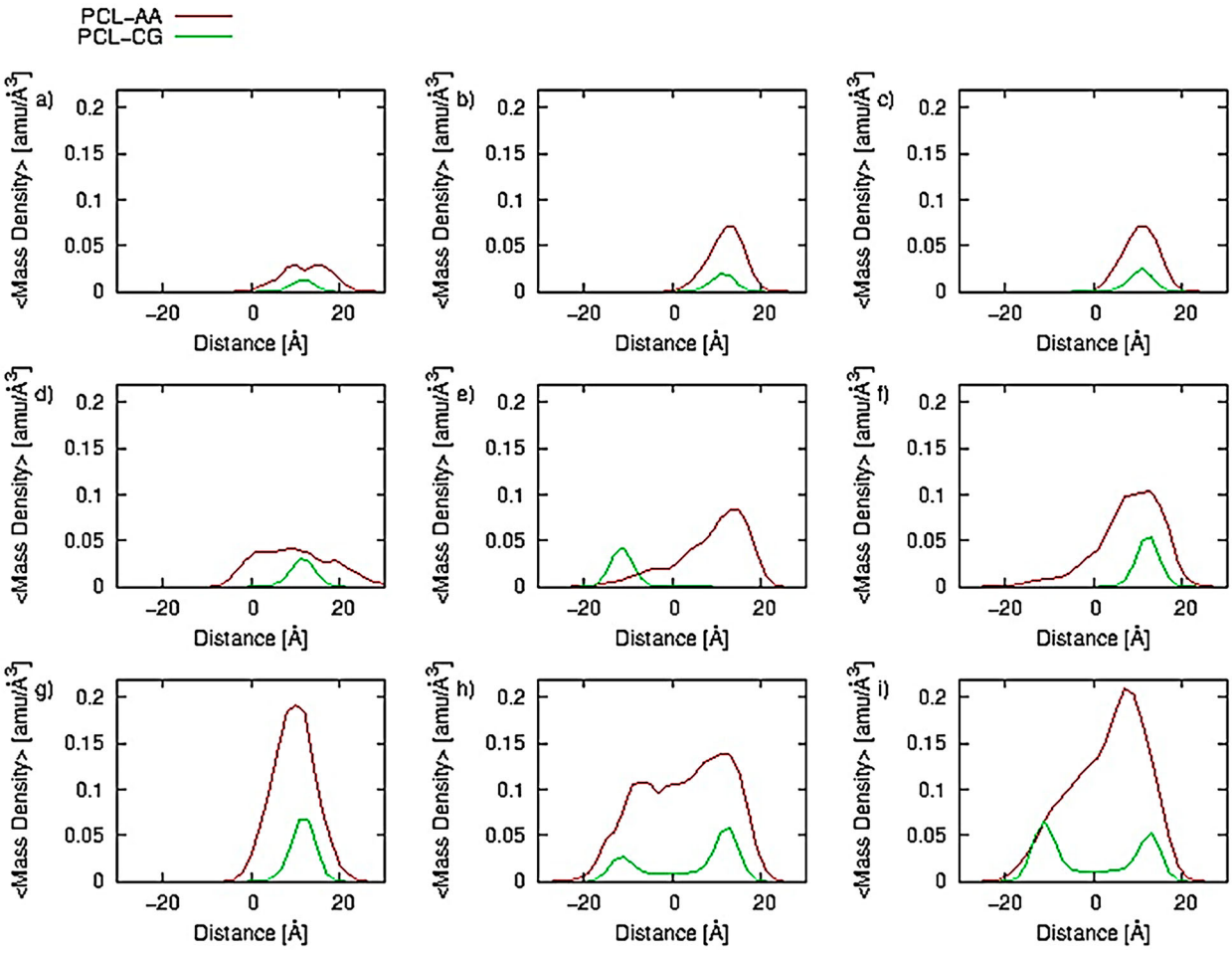

Figure 9. (Colour online) AA-CG average PCL mass density distributions of the PCL (green), water (cyan) and POPC (magenta) along the *Z*-axis of the simulation box, for the last 10 ns of simulations. (a) 5 PCL; (b) 8 PCL; (c) 10 PCL; (d) 13 PCL; (e) 17 PCL; (f) 22 PCL; (g) 30 PCL; (h) 44 PCL; (i) 58PCL.

The polar head groups of the membrane are highly solvated, acting as a barrier that impedes the movement of PCL chains to move towards water region. We see that this barrier exists for both short chains, in extended conformations or long, gathered-disordered chains that remain within the membrane, without crossing the membrane-water interface. However, the loose ends of intermediate chains, once they come in contact with the top portion of membrane's hydrocarbon chains, can overcome the hydrophilic barrier of the membrane's head groups. The area per lipid as a function of polymer chain length is shown in Figure 3(b). Here, we see that with the membrane thinning of intermediate chain lengths comes an increase in area per lipid. After an initial increase area per lipid values decrease for intermediate chains. For longer chains, the area per lipid tends to plateau after which area per lipid increases for 58 monomers PCL. Clearly, such a pattern indicates that with the thinning of the membrane at intermediate chain lengths comes an increase in the area per lipid. However, this trend does not hold at longer chain lengths. We next computed mass density profiles for the last 10 ns of each trajectory (Figure 4). As would be expected, the PCL chain in the membrane shifts the mass distribution of the membrane. For longer chains, the PCL polymer density spreads throughout the membrane, while the density of the membrane decreases with the increase of PCL chain length. Additional Supplementary Information and discussion concerning these all-atomistic simulations, the polymer conformation, and the membrane response are in Supplementary Figures 1–16.

Next, given the limited sampling time of the previous simulations, we decided to perform advanced sampling simulations of three representative chain lengths interacting with the phospholipid membrane. We performed three sets of metadynamics simulations with three different polymer chain lengths – short (5 monomers PCL), intermediate (17 monomers PCL), and long (58 monomers PCL) – interacting with a POPC phospholipid membrane. Two collective variables are used: the radius of gyration of the polymer chain and the centre of mass distance from the polymer chain to the centre of mass of the phospholipid headgroups. To summarise, we find a transition of the minimum energy state for the polymer chain at the interface moving to the centre of the hydrophobic core; we characterise this shift in minimum energy configuration/location of the chain with 2D metadynamics calculations as shown in Figure 5. Snapshots of the chain conformations in different energy wells as a function of chain length are shown in Figure 6. Further discussion is in the Supplementary Information and time dependence to show the convergence of free energy calculations is shown in Supplementary Figure 17(i)–(iii).

Next, we describe the results of coarse-grained molecular dynamics simulations performed for single polycaprolactone (PCL) chains of varying lengths interacting with a POPC membrane (Figure 7). We compare these results with all-atomistic simulations. We investigate the nature of PCL chains and POPC membrane conformational changes as a result of the interactions between PCL chains, POPC membrane and water. The last 100 ns R_g versus number of monomers (Figure 8 (a)) indicates that shorter chains (5,8,10,13,17 PCL) show similar behaviour in both AA and CG simulations. Intermediate and large chains follow irregular patterns of increase in R_g with a number of monomers, where CG values for R_g are much larger than AA analogue. A power fit for R_g as a function of N, $R_g(N) = 4.35N^{0.42}$, gives a scaling coefficient ν in the range $1/2 < 0.42 < 1/3$, a state between disordered coil and collapsed globule.

The last 100 ns R_e (Figure 8(b)) AA-CG comparison shows that shorter chains (5,8,10,13,17 PCL) are quite similar, but starting with 22 PCL, in AA simulation, R_e is decreasing with increasing chain length. In all-atomistic simulations, intermediate chains approach the POPC-water interface in a state of partial collapse, with a smaller R_e than shorter or longer chains. The CG power law fit, $R_e(N) = 13.87N^{0.35}$ gave a scaling coefficient close to 1/3, consistent with a polymer in a poor solvent. Membrane thickness shows a slight increase with numbers of monomers, while in AA simulation membrane thickness varies in a more irregular pattern (Figure 8(c)). The CG area per lipid (Figure 8(d)) is far below the all-atomistic area per lipid. Furthermore, the area per lipid is not affected by the presence of polymer chains. These results may be dependent on the finite size of the membrane as well as the method for parameterisation of the interaction between the CG PCL polymer and the CG phospholipids. Specifically, we used the mixing rule to describe the interaction between polymer and phospholipids. In order to further improve the present model, parameters could be refined such that agreement is found between all-atomistic and coarse grain surface tensions, when the polymer is solubilised in the membrane. Compared with AA simulations, PCL densities (Figure 9) are lower than AA densities. Further comparison between AA simulations CG simulations, such as the time evolution of the radius of gyration and end-to-end distance of the polymer chain, membrane thickness, area per lipid and surface accessible surface area, are shown in Supplementary Figures 18–33.

4. Summary

Herein we described and characterised the biophysical interactions between a model phospholipid membrane bilayer composed by POPC and single polycaprolactone chains of varying lengths. First, we characterised the equilibrium interfacial location of the polymer in the membrane after 150 ns all-atomistic MD simulations. We also characterised the shape of the polymer, using the radius of gyration. We find that the polymer shifts its behaviour from shorter to intermediate to longer chains, moving from the membrane-water interface to the hydrophobic core of the membrane. We also characterised the molecular tail order parameter of the POPC bilayer, showing that longer polymers display a greater disruption of the phospholipid tails. The interaction between the polymer and phospholipid tails consists of van der Waals attraction between polymer segments, the polymer and the membrane, as well as steric and electrostatic interactions between the PCL chain and the membrane, that tend to expand the polymer. It is found that short chains cause a membrane thinning, most likely due to a lateral pressure of the chain which sits near the interface, expanding the membrane. However, as the chain becomes longer the polymer prefers to sit inside the centre of the hydrophobic core of the membrane, which does not lead to a membrane thinning effect. Likely, the elasticity of the membrane is also affected by the presence of these polymer chains at the interface or the centre of the hydrophobic core of the membrane. However, this would need to be further characterised and would depend on the concentration of polymer interacting with the membrane.

In order to improve the sampling of the conformation of the polymer chain and characterise the interaction free energy in detail, we next utilised metadynamics, an accelerated sampling technique. The results confirm that the minimum in the free energy surface shifts from the membrane-water interface to the centre of the hydrophobic core of the membrane as a function of chain length. Likely, these results would also be concentration dependent on the number of polymers interacting with the hydrophobic membrane. Indeed, multiple polymers interacting with the membrane may porate and disrupt the membrane entirely due to aggregation of the hydrophobic polymer in the centre of the hydrophobic core of the polymer. However, this effect may depend on the chain length of the polymer, as suggested here in these large-scale atomistic simulations.

Following, coarse-grained simulations demonstrate the spreading behaviour of PCL in a lipid membrane. While the CG simulation results describe the trend in the conformations of and partitioning of PCL chains in the membrane, it did not capture the membrane thinning effects of the polymer on the membrane itself as were observed in the AA simulations. With further parameterisation of the interaction between the polymer chain and the membrane, likely these effects could be more accurately captured in the model presented within. Furthermore, in order to accurately characterise the effects of the polymer on the mechanical properties of the membrane in large-scale models, this interaction needs to be further investigated and refined. With a coarse-grained model that accurately captures membrane thinning effects of hydrophobic polymers, their cooperative interaction and their effects on the membrane can be predicted. These results can then be used to design polymer chain lengths and chemistries to optimise their interaction with cell membranes at the molecular level.

Acknowledgements

MD would like to thank Dr Alex Tzanov from CUNY High Performance Computing Center and Lei Huang from the Texas Advanced Computing Center.

Disclosure statement

No potential conflict of interest was reported by the authors.

Funding

This research was supported, in part, by the NSF through TeraGrid resources under grant number TG-CHE130099 and a grant of computer time from the City University of New York High Performance Computing Center under NSF Grants CNS-0855217, CNS-0958379 and ACI-1126113. S. M. L. acknowledges start-up funding received from College of Staten Island and City University of New York. S. M. L. would also like to acknowledge PRF grant 54235-DNI6, NSF Grant DMR-1506937 and NSF Grant DMR-1750694. This work was supported by the American Chemical Society Petroleum Research Fund [grant number 54235-DNI6]; Directorate for Mathematical and Physical Sciences [grant number DMR-1506937 and DMR-1750694].

References

[1] Kwon G, Kataoka K. Block copolymer micelles as long-circulating drug vehicles. Adv Drug Deliv Rev. 1995;16:295–309.
[2] Ahmed F, Discher DE. Self-porating polymersomes of PEG-PLA and PEG-PCL: hydrolysis-triggered controlled release vesicles. J Control Release. 2004;96:37–53.
[3] Cai S, Vijayan K, Cheng D, et al. Micelles of different morphologies – advantages of worm-like filomicelles of PEO-PCL in paclitaxel delivery. Pharm Res. 2007;24:2099–2109.
[4] Dash TK, Konkimalla VB. Polymeric modification and its implication in drug delivery: poly-ε-caprolactone (PCL) as a model polymer. Mol Pharm. 2012;9:2365–2379.
[5] Forrest ML, Yanez JA, Remsberg CM, et al. Paclitaxel prodrugs with sustained release and high solubility in poly(ethylene glycol)-b-poly (epsilon-caprolactone) micelle nanocarriers: pharmacokinetic disposition, tolerability, and cytotoxicity. Pharm Res. 2008;25:194–206.
[6] Liu SJ, Chiang FJ, Hsiao CY, et al. Fabrication of balloon-expandable self-lock drug-eluting polycaprolactone stents using micro-injection molding and spray coating techniques. Ann Biomed Eng. 2010;38:3185–3194.
[7] Izquierdo R, Garcia-Giralt N, Rodriguez MT, et al. Biodegradable PCL scaffolds with an interconnected spherical pore network for tissue engineering. J Biomed Mater Res Part A. 2008;85A:25–35.
[8] Rajagopal K, Mahmud A, Christian DA, et al. Curvature-coupled hydration of semicrystalline polymer amphiphiles yields flexible worm micelles but favors rigid vesicles: polycaprolactone-based block copolymers. Macromolecules. 2010;43:9736–9746.
[9] Qiao C; Zhao J; Jiang S; Ji X; An L; Jiang B. Crystalline morphology evolution in PCL thin films. J Polym Sci Part B: Polym Phys. 2005;43:1303–1309.
[10] Schulz M, Olubummo A, Binder WH. Beyond the lipid-bilayer: interaction of polymers and nanoparticles with membranes. Soft Matter. 2012;8:4849–4864.
[11] Nawaz S, Redhead M, Mantovani G, et al. Interactions of PEO–PPO–PEO block copolymers with lipid membranes: a computational and experimental study linking membrane lysis with polymer structure. Soft Matter. 2012;8:6744–6754.
[12] Hezaveh S, Samanta S, De Nicola A, et al. Understanding the interaction of block copolymers with DMPC lipid bilayer using coarse-grained molecular dynamics simulations. J Phys Chem B. 2012;116:14333–14345.
[13] Jeong B, Bae YH, Lee DS, et al. Biodegradable block copolymers as injectable drug-delivery systems. Nature. 1997;388:860–862.
[14] Geng Y, Dalhaimer P, Cai S, et al. Shape effects of filaments versus spherical particles in flow and drug delivery. Nat Nanotechnol. 2007;2:249–255.
[15] Loverde SM, Klein ML, Discher DE. Nanoparticle shape improves delivery: rational coarse grain molecular dynamics (rCG-MD) of taxol in worm-like PEG-PCL micelles. Adv Mater. 2012;24:3823–3830.
[16] Laio A, Parrinello M. Escaping free-energy minima. Proc Natl Acad Sci. 2002;99:12562–6.
[17] Torrie GM, Valleau JP. Nonphysical sampling distributions in Monte Carlo free-energy estimation: umbrella sampling. J Comput Phys. 1977;23:187–199.
[18] Darve E, Rodriguez-Gomez D, Pohorille A. Adaptive biasing force method for scalar and vector free energy calculations. J Chem Phys. 2008;128:144120:1–144120:13.
[19] Loverde SM. Molecular simulation of the transport of drugs across model membranes. J Phys Chem Lett. 2014;5:1659–1665.
[20] Drenscko M, Loverde SM. Characterisation of the hydrophobic collapse of polystyrene in water using free energy techniques. Mol Simul. 2017;43:234–241.
[21] Vanommeslaeghe K, Hatcher E, Acharya C, et al. CHARMM general force field: a force field for drug-like molecules compatible with the CHARMM all-atom additive biological force fields. J Comput Chem. 2010;31:671–690.
[22] Brooks BR, Brooks III CL, Mackerell Jr. AD, et al. CHARMM: the biomolecular simulation program. J Comput Chem. 2009;30:1545–1614.
[23] Jorgensen WL, Chandrasekhar J, Madura JD, et al. Comparison of simple potential functions for simulating liquid water. J Chem Phys. 1983;79:926–935.
[24] Lee S, Tran A, Allsopp M, et al. CHARMM36 united atom chain model for lipids and surfactants. J Phys Chem B. 2014;118:547–556.
[25] Kale L, Skeel R, Bhandarkar M, et al. NAMD2: greater scalability for parallel molecular dynamics. J Comput Phys. 1999;151:283–312.
[26] Phillips JC, Braun R, Wang W, et al. Scalable molecular dynamics with NAMD. J Comput Chem. 2005;26:1781–1802.
[27] Martyna GJ, Tobias DJ, Klein ML. Constant-pressure molecular-dynamics algorithms. J Chem Phys. 1994;101:4177–4189.
[28] Darden T, York D, Pedersen L. Particle mesh Ewald – an n.log(n) method for Ewald sums in large systems. J Chem Phys. 1993;98:10089–10092.
[29] Shinoda W, DeVane R, Klein ML. Zwitterionic lipid assemblies: molecular dynamics studies of monolayers, bilayers, and vesicles using a new coarse grain force field. J Phys Chem B. 2010;114:6836–6849.
[30] Plimpton S. Fast parallel Algorithms for short-range molecular dynamics. J Comput Phys. 1995;117:1–19.
[31] Martyna GJ, Klein ML, Tuckerman M. Nose–Hoover chains – the canonical ensemble via continuous dynamics. J Chem Phys. 1992;97:2635–2643.
[32] Deserno M, Holm C. How to mesh up Ewald sums. I. A theoretical and numerical comparison of various particle mesh routines. J Chem Phys. 1998;109:7678–7693.
[33] Henin J, Fiorin G, Chipot C, et al. Exploring multidimensional free energy landscapes using time-dependent biases on collective variables. J Chem Theory Comput. 2010;6:35–47.
[34] Fiorin G, Klein ML, Hénin J. Using collective variables to drive molecular dynamics simulations. Mol Phys. 2013;111:3345–3362.
[35] Bussi G, Gervasio FL, Laio A, et al. Free-energy landscape for beta hairpin folding from combined parallel tempering and metadynamics. J Am Chem Soc. 2006;128:13435–13441.
[36] Ensing B, De Vivo M, Liu ZW, et al. Metadynamics as a tool for exploring free energy landscapes of chemical reactions. Acc Chem Res. 2006;39:73–81.